Available online at www.sciencedirect.com
ScienceDirect
PERGAMON
Acta Astronautica 60 (2007) 873–879
ACTA ASTRONAUTICA
www.elsevier.com/locate/actaastro

Equivalence principle test with microscope: Laboratory and engineering models preliminary results for evaluation of performance

Ratana Chhun*, Danya Hudson, Patrick Flinoise, Manuel Rodrigues, Pierre Touboul, Bernard Foulon

Office National d'Etudes et de Recherches Aérospatiales, (ONERA), B.P. 72, 92322 Châtillon, France

Received 15 February 2006; accepted 6 November 2006
Available online 10 January 2007

Abstract

MICROSCOPE is a space mission, scheduled for a launch in 2010, which aims to verify the equivalence principle (EP) with an accuracy of 10^{-15}, over a hundred times better than what has been realized on Earth today. The EP test is based on the measurement of the electrostatic forces to be applied on each test mass of two concentric inertial sensors, in order to maintain these two masses on the same gravitational trajectory. The instrument formed by these two sensors is called a differential accelerometer. On board the MICROSCOPE satellite, two instruments will embark: one for the test itself, and the other as a performance reference. The first of several mechanical models for this instrument have been manufactured. Each is designed to demonstrate a specific part of the development. Associated to the differential accelerometer, a performance software has also been developed. In order to reach the required performance, an in-orbit calibration phase is planned to improve the knowledge of the geometrical dissymmetries and orientation mismatches. Detailed finite element thermal models of the accelerometers have been realized and currently provide information on the behavior of accelerometer parts in response to the satellite thermal perturbations.

1. The equivalence principle

For centuries, experiments have alleged the universality of free fall, from which the equivalence between inertial mass and gravitational mass originates. At the beginning of the 20th century, Einstein set this property as a postulate for general relativity which requires that all bodies acquire the same acceleration rate in the same uniform gravity field regardless of inertial mass or intrinsic composition. Since then general relativity has become, along quantum mechanics, one of the bases of physics as we know it. But the last three decades have seen the emergence of unification theories which aim to merge these two fundamentally separated theories, and predict the existence of a fifth interaction force which would appear as a violation of the equivalence principle (EP). Up to now experiments have verified it to a precision of a few 10^{-13} [1], but these ground-based experiments are limited to this order of precision because of disturbances inherent to the

* Corresponding author.
E-mail addresses: ratana.chhun@onera.fr (R. Chhun), danya.hudson@onera.fr (D. Hudson), patrick.flinoise@onera.fr (P. Flinoise), manuel.rodrigues@onera.fr (M. Rodrigues), pierre.touboul@onera.fr (P. Touboul), bernard.foulon@onera.fr (B. Foulon).

0094-5765/$ - see front matter © 2006 Elsevier Ltd. All rights reserved.
doi:10.1016/j.actaastro.2006.11.002

environment, such as seismic noise and human activity, or a short free-fall duration. Since unification theorists expect a violation to be beyond the 10^{-13} [2], the future of such experiments looks toward space.

2. The MICROSCOPE mission

CNES by way of its microsatellite line has selected and currently funds the MICROSCOPE mission in collaboration with ONERA and OCA. The mission intends to test the EP at the level of 10^{-15}, by placing in 2010 specific space accelerometers called SAGE in free fall around the Earth. The experience of ONERA in the accelerometer field, exhibited by previous missions such as CHAMP and GRACE [3], will however be challenged by the precision requirements and by the nature of the test. In addition to levitating and controlling two proof masses using electrostatic forces, the accelerometers will have to maintain them in the exact same gravity field. To achieve this, a differential accelerometer featuring two concentric cylindrical proof masses is under development. The shape, when compared to the parallelepipedic proof masses used in previous instruments, presents many challenges, but is necessary to minimize the effect of the gravity gradient as it is as close as possible to the ideal but technically unusable sphere shape. Maintaining their centering along the same orbit is also a key issue. The satellite will also make use of a drag-compensation system, to ensure a true free fall, while conforming to the restrictions on size, mass and power consumption defined by the CNES microsatellite program.

The space EP test will benefit from low-environment noise due to a very weak vibration level further reduced by the drag-compensation system operation, from a long free-fall duration and thus a long data integration time for better signal to noise ratio, and from a diversity of measurement frequencies ranging from the orbital frequency in inertial pointing mode to higher frequencies when combined with an additional spin of the satellite, for a projected range between 10^{-4} and 10^{-2} Hz. Two differential accelerometers will embark on the satellite, the first one featuring two proof masses made of the same material and used as a purely performance testing instrument and reference, the second one featuring masses made of different materials to perform the EP test. In the end a differential measurement of the accelerations required to control the two masses on their gravitational trajectory shall be performed along the cylinder axis. For the reference instrument, a null difference is expected, but for the EP test instrument, a difference of signal should translate as a violation of the EP.

Currently halfway through the whole instrument development, this article will describe its overall design and the activities involved to confirm the design, such as mechanical models, performance software, finite element thermal models and analyses for the in-orbit calibration phase. The paper will then present the first tests and analyses, the results and their impact on the performance.

3. Instrument description

One inertial sensor consists of a mechanical assembly mounted around an electrostatically levitated mass and associated control electronics. In the case of SAGE, two inertial sensors are positioned to give their proof masses the same center of gravity, to form one differential accelerometer. To obtain such a configuration the masses are cylindrical, with carefully machined dimensions, to approximate spherical moments of inertia, in order to reduce the gravity gradient disturbing effects. Each mass is maintained centered in six degrees of freedom by means of electrostatic forces from a surrounding cage of electrodes in gold-coated silica (Fig. 1). The only physical contact between the mass and its surrounding cage is a 5 μm diameter gold wire, which is necessary to maintain its electrical charge stable, and also applies a high-frequency voltage used for the capacitive position sensing. The electrodes, working in pairs, are used for both displacement detection, by differential capacitive measurement, and position control, by electrostatic force actuation. Position sensing and actuation are designed to be linear along the instrument sensitive axis, the cylinder axis, in such a way to permit fine frequency signal analysis of the data.

Stops set at each end of the mass limit its range of free motion to avoid a short circuit between the mass

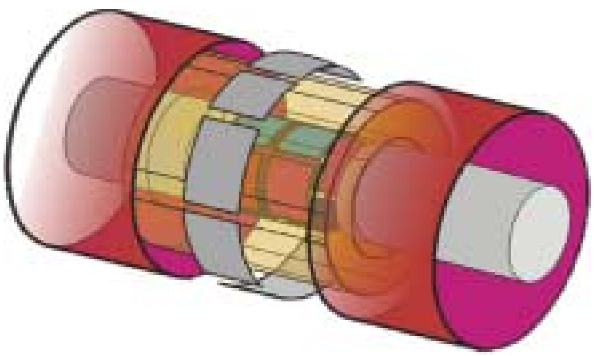

Fig. 1. Electrode configuration, axial translation and rotation control without the proof mass, radial translation and rotation control within.

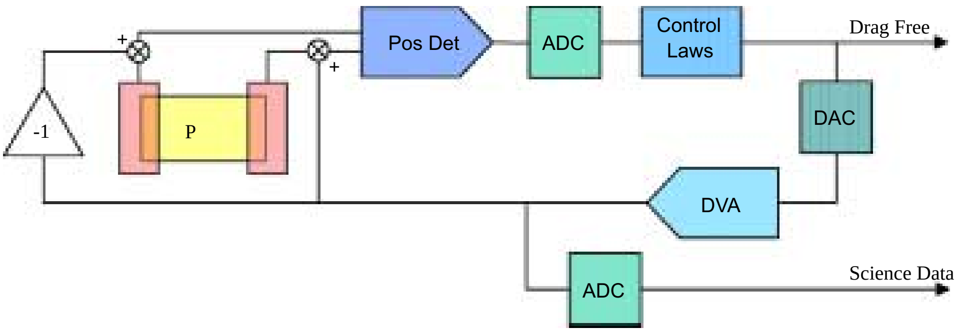

Fig. 2. Control-loop scheme of the EP test axis.

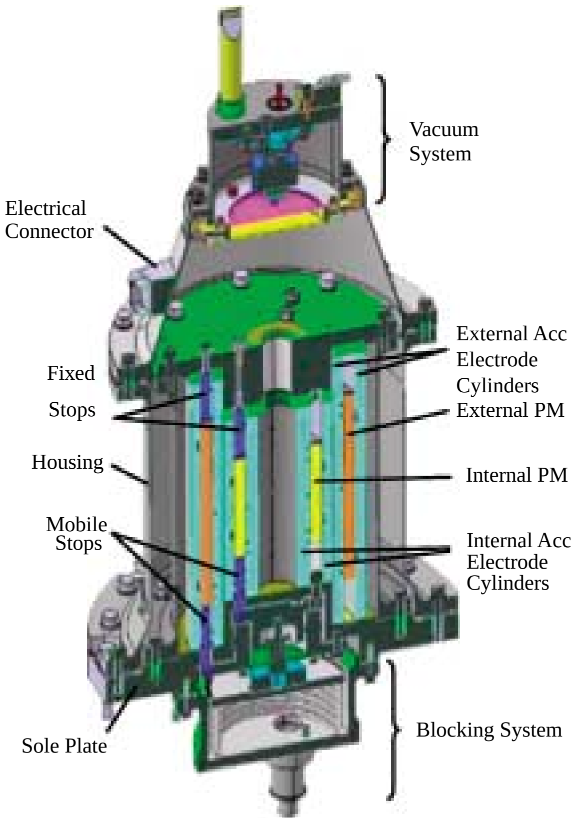

Fig. 3. Cut view of the sensor core.

and electrodes and stress on the gold wire. A blocking mechanism completes the mechanical core by pressing one of the sets of stops onto the mass, blocking it during launch and releasing it once in orbit. All cylindrical parts of the sensor core, including also an invar magnetic shielding envelope, are finely aligned to 10^{-3} rad during integration and assembly by mounting them on a unique base plate also made of invar. Once complete and enclosed, the interior of the instrument is placed under vacuum. A getter material device is mounted on the top of the sensor to maintain the pressure below 10^{-5} Pa.

The electronics component includes two separate modules for each sensor, the front end electronics unit and the interface control unit, the former containing the analog electronics such as detection and voltage actuation functions and the analog-to-digital and digital-to-analog converters, the latter containing the digital electronics of the six position servo-control channels (Fig. 2), the combination functions to convert between degree of freedom and specific electrode signals and the satellite interface.

The two differential accelerometers on the satellite are identical except for the material of their masses. The reference has two platinum–rhodium masses while the test instrument has an inner platinum–rhodium mass and an outer titanium alloy mass (Fig. 3).

4. Measurement principle

The science measurements of one sensor are the applied voltages needed to maintain the mass centered with respect to its electrode cage, to compensate for both gravity and surface forces on the satellite. The differential measurement between the two inertial sensors is then expressed as follows:

$$\frac{\hat{F}_A}{m_{\mathrm{I}_A}}-\frac{\hat{F}_B}{m_{\mathrm{I}_B}}\approx\begin{cases}\frac{1}{2}(K_A-K_B)(\ddot{x}_A-g_A+\ddot{x}_B-g_B) & \text{(a)}\\ \quad +(x''_A-x''_B)+2\Omega(x'_A-x'_B) & \\ \quad +(\Omega\times\Omega+\Omega')(x_A-x_B) & \text{(b)}\\ \quad -\left(\frac{m_{\mathrm{g}_A}}{m_{\mathrm{I}_A}}+\frac{m_{\mathrm{g}_B}}{m_{\mathrm{I}_B}}\right)\left(\frac{g_A-g_B}{2}\right) & \text{(c)}\\ \quad -\left(\frac{F_{\mathrm{P}_A}}{m_{\mathrm{I}_A}}-\frac{F_{\mathrm{P}_B}}{m_{\mathrm{I}_B}}\right) & \text{(d)}\\ \quad -\left(\frac{m_{\mathrm{g}_A}}{m_{\mathrm{I}_A}}-\frac{m_{\mathrm{g}_B}}{m_{\mathrm{I}_B}}\right)\left(\frac{g_A+g_B}{2}\right) & \text{(e)}\\ \quad +E(F_A)-E(F_B)+E_{\mathrm{n}_A}-E_{\mathrm{n}_B}. & \text{(f)}\end{cases}$$

Term (e) is the signal to be detected in case of EP violation where m_g and m_I are, respectively, the gravitational mass and the inertial mass of each material. The other expressions are maintained weak during the space experiment. The common acceleration $\ddot{x}$ in expression (a) and the satellite angular velocity Ω and acceleration Ω' in expression (b) are at low levels of a few $10^{-8}\,\mathrm{m/s^2}$, $10^{-6}\,\mathrm{rad/s}$ and a few $10^{-6}\,\mathrm{rad/s^2}$, respectively, thanks to the drag free and attitude control system. A calibration phase will also decrease noticeably the components of the $(K_A - K_B)$ scale factor differential matrix by matching and improve the knowledge on the relative position $(x_A - x_B)$ with respect to the instrument referenced frame. The servo-control maintains the relative motion of the two masses constant by keeping each of them motionless with respect to the common reference of the electrode cylinders fixed on the base plate. The Earth's gravity gradient effects $(g_A - g_B)$ in expression (c) are limited by the concentricity of the masses and those due to the self-gravity gradient of the satellite by the choice on their shape and dimensions. F_p in expression (d) represents non-gravitational parasitic accelerations such as radiation pressure and radiometer effect. Finally, expression (f) gathers the instrument noise sources including measurement electronics noise E_n and bias and scale factor thermal sensitivities $E(F)$.

5. Mechanical models

During the development process, several sensor models have been or will be manufactured in order to test different feasibility and mechanical aspects of the final flight models.

The first already existing model is the prototype. Its main objective is to demonstrate on ground, under nominal gravity, the feasibility of levitating a cylindrical mass with an arrangement of electrodes nearly identical to the MICROSCOPE configuration [4]. This model features only one inertial sensor and has specific analog servo-control electronics used to produce a strong electrical field in order to generate sufficient electrostatic pressures to sustain the $1g$ acceleration. The mass is made of 14 g of silica instead of over 300 g of platinum or titanium, and even with a reduced distance of 10 μm between the electrodes and mass, still requires 400 V on the vertical axis electrodes to counteract gravity.

The second model is the vibration test model. It is almost identical to the flight model, with fewer engravings and less cabling since its purpose is to establish the integration processes and to test the general behavior of the core mechanics under vibration conditions. It does not feature the vacuum pump and is not functional.

The engineering model is currently being manufactured, with integration to be completed in September 2005. This model is identical to the flight model except for its masses of silica. Since this model is destined to ground testing, it requires lighter masses for levitation, as well as electronics and cabling modified for the $1g$ environment.

Fig. 4. Vibration model under sinus vibration test.

The qualification model, identical to the flight model, will be used for vibration, thermal and EMC testing and will operate during free-fall tests in the ZARM drop tower.

In the end the two flight models will undergo another campaign of more limited vibration tests and a calibration which will cover as many parameters as possible on ground. The development of the instrument will conclude on a final drop test in the ZARM free-fall tower prior to the integration into the satellite and the launch.

6. Tests and outputs on the mechanical models

The levitation of the mass of the prototype is under way, but while the vertical lift functions and is well controlled, a large electrostatic stiffness presents difficulties for the control of the horizontal axes. This stiffness is due to the quality of the horizontality of the instrument setting in that a projection of g on the horizontal axis requires higher voltage to be applied on the appropriate electrodes. However, the voltages applied to other electrodes including that for vertical lift also contribute to the stiffness. Unfortunately the higher the voltage is, the higher the stiffness also. This difficulty inherent to ground testing is currently under investigation.

The vibration model has been integrated with high accuracy, its electrode cylinders centered with a few μm precision. The testing has commenced with sinus vibrations for now up to the $10g$ level (Fig. 4). The mechanics

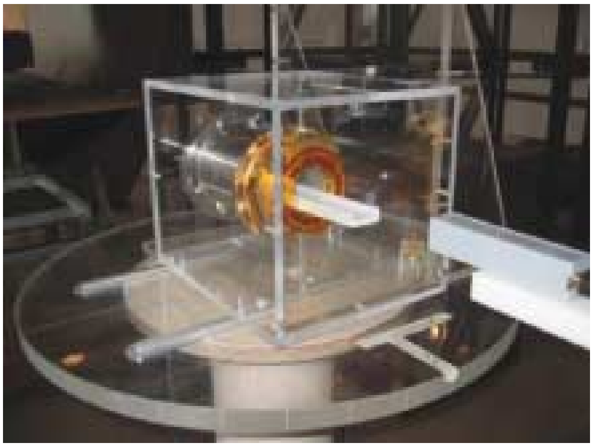

Fig. 5. Engineering model accelerometer under magnetic field test at Intespace/CNES facilities.

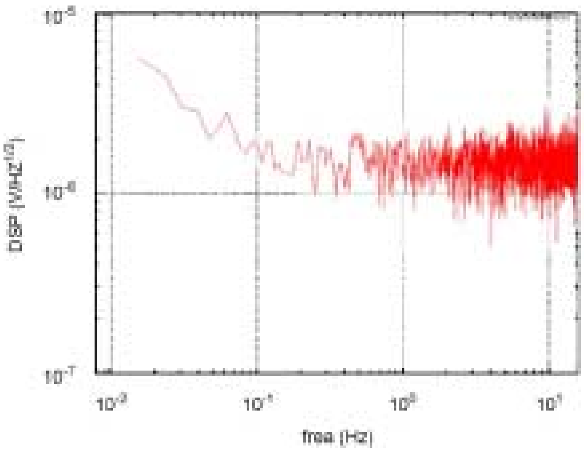

Fig. 6. Drive voltage amplifier noise $< 1.2\,\mu V/Hz^{1/2}$.

displayed no physical damage; however, the results are still being examined. The natural frequencies of the sensor unit have been identified above 300 Hz and match those predicted by the finite element mechanical models described in the “Finite Element Models” section.

One invar magnetic shielding envelope to be used in the qualification model integration has also been put under magnetic tests, performed in both Intespace/CNES and ONERA facilities. Two different aspects of the shielding were tested, the coefficient of attenuation between the exterior exciting magnetic field and the measured field inside the shielding, and the influence of the invar parts on surrounding elements inside the satellite, especially the influence of the shielding of one sensor unit on the other.

The CNES campaign consisted in placing the shielding at the center of a dedicated lab with compensation for the Earth’s magnetic field, and the possibility of generating any exciting field (Fig. 5). The measured attenuation factors of 10 along the axial axis and 25 along the radial differ due to the cylindrical geometry. These results are satisfactory when compared to the value of 7 considered in the current version of the error budget.

Another campaign led in ONERA consisted in mapping first the Earth’s magnetic field in the selected clean lab, then the induced field around the shielding placed in that same room. These measurements show that the influence of the presence of one invar shielding is very weak at distances of about 10 cm, the distance between the two instruments onboard the satellite, and only slightly changes the orientation of the field but does not increase its value.

The electronics of the engineering model are currently under test. All functionalities have been successfully tested but performance results are still being analyzed. Fig. 6 shows a noise measurement of the voltage actuators. In June 2005, thermal tests were also conducted in CNES facilities to investigate the behavior of the power supplies and the different functions of the electronics loops with respect to temperature variations. One important result from this campaign is the temperature transfer functions between the electronics sensitive components and the mounting surface of the unit. These will allow computation of the actual thermal characteristics of the inertial sensor operation.

7. The error budget

The instrument error budget is now computed with more than one hundred components. The program has been developed to detail all the specifications of the mechanics configuration and machining, the electronics design and the environmental disturbances required to meet the performance level of a few $10^{-12}\,m/s^2/Hz^{1/2}$ required to attain a 10^{-15} accuracy of the EP test. From these parameters the program computes the expected bias and noise from available physical models or experimental characterizations of each implied physical phenomenon. An alternative version of the program takes as inputs the actual values measured on each inertial sensor, such as geometrical dissymmetries, machining accuracies and electronics noise. This latter version reflects the actual performance of the instrument rather than the specification defined in the earlier one, and is seen as a tool for the data analysis of the mission. By computing the acceleration disturbance contributors, this software is especially useful for determining the critical parameters to investigate primarily. For instance,

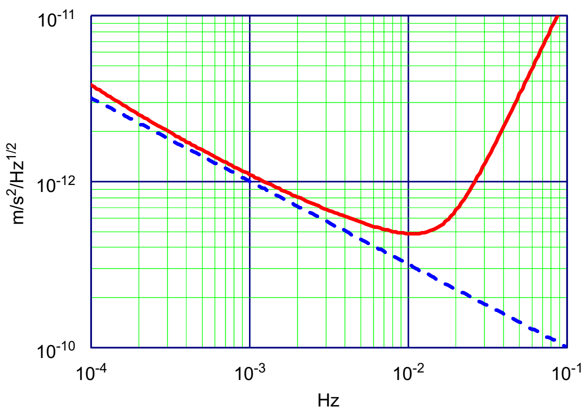

Fig. 7. Error budget resolution of the EP outer sensor (continuous line) and contribution of the gold wire damping (dashed line) along the sensitive axis.

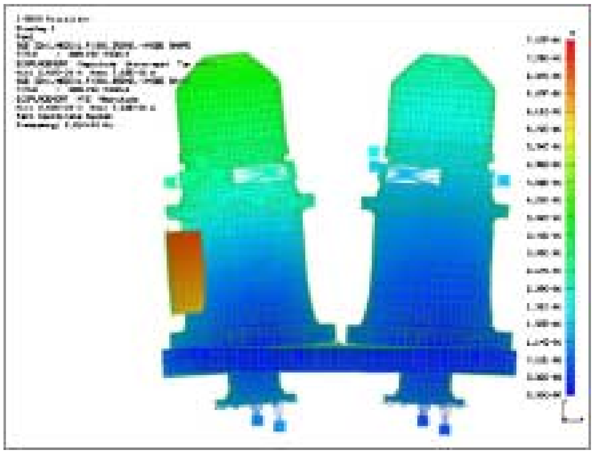

Fig. 8. Finite element model identifying the first mode at 301.4 Hz.

mass damping clearly stands out as the major noise contributor thus pointing to the source of this damping, the gold wire as a critical component to reach the targeted performance (Fig. 7). In the present design, this gold wire is 2.5 cm long and has a 5 μm diameter, the handling of which is a critical step of the integration process.

8. Finite element models

Thermal and mechanical finite element models have been developed to analyze the behavior of the sensor unit under various types of temperature variations and various types of physical stress.

The thermal model is developed to anticipate the thermal transfer functions between the physical interfaces and the masses, internal instrument core or electronics.

Two models were actually created: a detailed model gives fine behavior of each unit while an approximation version is integrated by CNES into their satellite model. The complexity of the latter remains sufficiently detailed to determine gradients of temperature along the axes of the mass in order to compute the radiation pressures and the radiometer effects.

The mechanical model has several purposes:

- To determine the natural frequencies of the mechanical core and verify that they are all above the frequency limit of 300 Hz authorized for the launcher.
- To evaluate the resistance to the sine and random vibrations, and to the shock and quasi-static shock, encountered by the sensor during launch or during free-fall tests, in all the possible configurations of the mass, blocked or unblocked.
- To study the possible deformations of the ensemble or parts of it under various extreme conditions, either by vibration, shock or thermoelasticity within a temperature range, between −20 and 100 °C.
- To verify the insulation of the ensemble from the getter ring whose temperature can reach 800 °C once activated.

This ongoing study has confirmed such points as the natural frequencies being above 300 Hz and the isolation of the getter heat (Fig. 8).

9. Calibration study

The geometrical inaccuracies of all the parts of the two sensor units can be the source of dissymmetries, between either the two masses of the same differential accelerometer or the source of instabilities between one sensor and the satellite, referenced by its star tracker. Consequently, in addition to specifications on the mechanics manufacturing, a calibration phase to be performed in orbit is currently under study [5]. This study identifies three kinds of parameters to calibrate: misalignments, couplings and scale factors. Several scenarios are thus defined in which the satellite and the masses are oscillated along or about their axes for a duration sufficient to extract the relevant calibration signal from the overall environmental noise (Fig. 9).

Once more accurately evaluated in orbit, the calibrated parameters can be corrected in the measurement, leaving only a fraction of its original influence and thus increasing the precision of the measurement to that required for the 10^{-15} objective.

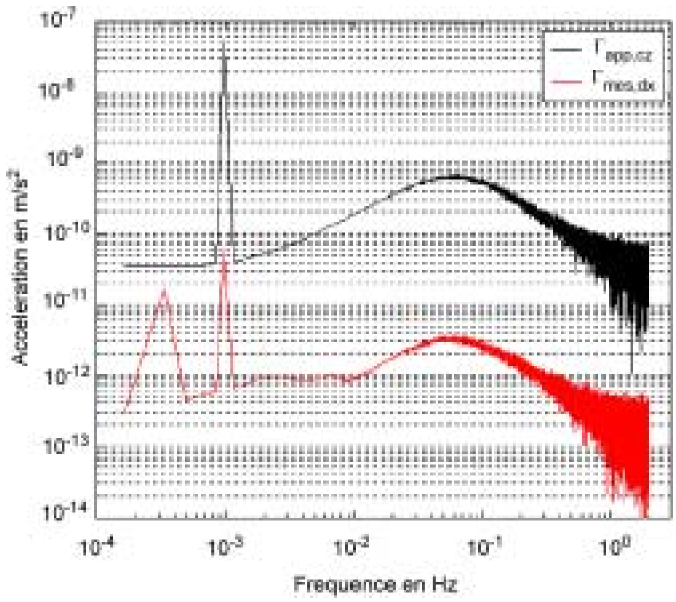

Fig. 9. Calibration simulation, after sinusoidal oscillation of the accelerometer at a specific frequency, and measurement of the differential acceleration, the ratio of the two peaks gives the value of the calibrated parameter.

10. Conclusion

The development of the SAGE instruments is currently in phase B and approaching its preliminary design review. All the tests already performed indicate a good progress toward the expected performance although much work remains to be done. Among the studies and tests in preparation for the next few months are the free-fall tests at ZARM and a simulation of the complete mission.

In the context of the calibration, a simulation of the control-loop process including the instrument, the satellite and the environment is being developed in order to test the efficiency of the scenarios defined in the study, and investigate alternative methods of calibration [6].

References

[1] S. Baessler, B.R. Heckel, E.G. Adelberger, J.H. Gundlach, U. Schmidt, H.E. Swanson, Improved test of the equivalence principle for gravitational self-energy, Physical Review Letters 83 (18) (1999) 3585–3588.

[2] T. Damour, F. Piazza, G. Veneziano, Violations of the equivalence principle in a dilaton-runaway scenario, Physical Review D 66 (4) (2002) 046007.

[3] M. Rodrigues, B. Foulon, F. Liorzou, P. Touboul, Flight experience on CHAMP and GRACE with ultra-sensitive accelerometers and return for LISA, Classical and Quantum Gravity 20 (2003) 291–300.

[4] D. Hudson, R. Chhun, P. Touboul, Development of a differential accelerometer to test the equivalence principle in the microscope mission, Acta Astronautica 57 (2005) 341–347.

[5] G. Pradels, Etalonnage en orbite d'Accéléromètres Ultrasensibles pour un Test du Principe d'Equivalence à 10^{-15}, Ph.D. Thesis, Univ. Paris VI Pierre et Marie Curie, 2003.

[6] E. Guiu, M. Rodrigues, P. Touboul, Étalonnage de l'Instrument de la Mission MICROSCOPE, in Proceedings Journées Doctorales et Nationales du GDR MACS JDMACS-JNMACS 2005, INSA Lyon, Lyon, September 2005.